

Directed evolution algorithm drives neural prediction

Yanlin Wang^{1,2}, Nancy M Young^{3,4,5}, Patrick C M Wong^{1,2*}

¹Brain and Mind institute, The Chinese University of Hong Kong, Hong Kong SAR, China

²Department of Linguistics and Modern Languages, The Chinese University of Hong Kong, Hong Kong SAR, China

³Division of Otolaryngology, Ann & Robert H. Lurie Children's Hospital of Chicago, Chicago, Illinois, United States.

⁴Department of Otolaryngology Head & Neck Surgery, Feinberg School of Medicine, Northwestern University, Chicago, Illinois, United States.

⁵Knowles Hearing Center, Department of Communication Sciences and Disorders, Northwestern University, Evanston, Illinois, United States.

***Corresponding Authors:**

Patrick C M Wong, PhD

Brain and Mind institute, Department of Linguistics and Modern Languages, The Chinese University of Hong Kong

Email: p.wong@cuhk.edu.hk

Abstract

Neural prediction offers a promising approach to forecasting the individual variability of neurocognitive functions and disorders and providing prognostic indicators for personalized invention. However, it is challenging to translate neural predictive models into medical artificial intelligent applications due to the limitations of domain shift and label scarcity. Here, we propose the directed evolution model (DEM), a novel computational model that mimics the trial-and-error processes of biological directed evolution to approximate optimal solutions for predictive modeling tasks. We demonstrated that the directed evolution algorithm is an effective strategy for uncertainty exploration, enhancing generalization in reinforcement learning. Furthermore, by incorporating replay buffer and continual backpropagate methods into DEM, we provide evidence of achieving better trade-off between exploitation and exploration in continuous learning settings. We conducted experiments on four different datasets for children with cochlear implants whose spoken language developmental outcomes vary considerably on the individual-child level. Preoperative neural MRI data has shown to accurately predict the post-operative outcome of these children within but not across datasets. Our results show that DEM can efficiently improve the performance of cross-domain pre-implantation neural predictions while addressing the challenge of label scarcity in target domain.

Introduction

Neural prediction—utilizing brain data to predict health and behavioral characteristics such as mental health and developmental status—is an area of increasing interdisciplinary research and emerging clinical applications. This application relies fundamentally on a computational framework that leverages advances in machine learning and neuroscience to translate neural data into clinically meaningful forecasts. With the rapid expansion of neuroscience and the advance of machine learning algorithms, there is a considerable need to deliver neural predictive models with individual-level precision to inform clinical decision-making.

However, AI applications designed for clinical use in medical decision-making rarely consider the question of whether prediction accuracy will be maintained when the model is faced with new, unseen data [1-3]. The growing number of medical algorithms already in use that were trained on limited clinical data was recently highlighted in Nature. [4] The author points out that the accuracy of many medical AI enabled prediction models is at risk of degrade because they rely on a single training dataset. In addition, there are no U.S. regulations requiring medical centers to evaluate prediction accuracy when AI medical applications are used for local populations. Testing AI models at the local level before adoption is costly and therefore may not be feasible. Failure of prediction models to perform accurately is an important issue that undermines the potential and safely of neural prediction in real-world application. Therefore, AI system improvement in generalizability to increase accuracy and cost-effectiveness is critical for neural prediction in real-world applications.

Medical AI-based applications must maintain prediction accuracy when encountering heterogenous data from differing populations. Population heterogeneity, variations in data collection, and the use of different assessment tools pose significant challenges for multi-center validation across diverse populations, largely due to shifts in underlying features and labels. To address domain shifts, some researchers advocate developing a foundation model

based on a large, diverse dataset, where a pretraining model can be fine-tuned on a smaller, domain-specific dataset. [4-6] Despite the high promise of this pretraining strategy in supervised learning, its clinical application proves more challenging due to the significant differences between scarce domain-specific medical datasets and general-purpose pretraining datasets, as well as the high computational costs of this approach. [7-9] In practice, only a small amount of labelled data and a much larger amount of unlabelled data is typically available for reasons such as limitations in data collection. [10, 11] Consequently, the inherent uncertainties of clinical medicine data significantly impact model generalization, posing challenges for AI-based medical applications, particularly in children's healthcare where rapid brain development and varying assessment tools introduce more heterogeneity. [12-14]

Domain adaptation methods are designed to enable a model trained on one source of data to adapt to data with differing characteristics. These methods have received increasing attention in computer vision, [15] natural language processing, [16] and medical image fields. [12] For example, domain adaptation methods (e.g., adversarial and contrastive learning methods) focus on learning transferable and invariant feature representations across the source and target domains, thereby enabling effective model adaptation from the source domain to the target domain. [17, 18] However, current domain adaptation methods have limitations: they primarily focus on learning transferable and invariant representations across domains but often fall short in addressing both feature and label shift challenges. [19, 20] Overcoming these limitations is even more important and challenging in neural prediction as compared to disease identifications from medical data such as imaging. Neural prediction, especially in children, often involves data that dynamically shifts due to developmental changes and the need to forecast uncertain outcomes. Thus, while domain adaptation mitigates domain shift, it

fails to address true out-of-distribution (OOD) challenges where target data deviates significantly from a model’s training set. [20, 21]

Generalization in reinforcement learning (RL) is a model’s ability to perform well when presented with real world data that differs from training data. Medical AI and autonomous driving performance underscore the vulnerability of RL to minor changes in data, emphasizing the need to address this issue before deploying RL in real-world applications. [22-25] This has become a key focus of ongoing research, with recent benchmarks like OpenAI’s ChatGPT-o1 significantly advancing the state-of-the-art in AI reasoning by testing AI system’s ability to generalize to new tasks and align with human feedback. [26-28] Unlike large language models, which are highly tolerant of semantic uncertainty, constructing an efficient feedback mechanism in medical applications remains challenging, as most existing algorithms may struggle to explore efficiently under low-entropy scenarios. Therefore, enhancing the efficiency of uncertainty exploration techniques in which AI systems recognize and manage data uncertainty is critical for enhancing RL generalization. [29, 30]

Directed evolution is a method that mimics natural Darwinian evolution in a more targeted and fast manner, effectively applying cycles of selection and mutation to generate desired variants. [31-34] It is widely applied to protein engineering and uses ML to create libraries of data and selects proteins with specific properties. Direct evolution predicts outcome via an iterative process by computer simulation which reduces time and cost of lab experimentation. Inspired by this principle of directed evolution, we propose the directed evolution model (DEM) to optimize uncertainty exploration strategies by iteratively applying selection and evolution (e.g., mutation) to OOD data. The overarching goal of DEM is to develop an intelligent model capable of rapidly adapting to new, unseen data. Specifically, our main contributions can be summarized as follows: First, we expand the evolutionary computational model for directed evolution to address both domain shift and label scarcity issues. The

transition from screening to evolving learning facilitates the integration of evolutionary strategies into a computational framework that can easily be extended to a large-scale data and reduce the computation consumption. [33] Next, DEM can provide a unique solution for uncertainty exploration through mimicking the trial-and-error process of directed evolution. This approach can leverage pseudo-labelling strategies to address label scarcity, while utilizing evolutionary strategies to guide the agent’s exploration, reduce uncertainty and facilitate more targeted, rapid adaptation. Then, replay buffer and continual backpropagate approaches were integrated to achieve a better trade-off between exploitation and exploration. Finally, a confidence calibration approach was introduced to enhance the efficiency of the screening and evolving process.

In this study, we apply our novel DEM framework to neural prediction of children with cochlear implant (CI) with a multi-center setting. The cohort constitutes an exceptional test case for model generalization assessment due to multifactorial heterogeneity spanning biological, demographic, clinical and technical domains. First, the etiology and pathogenesis of hearing loss are often unknown, and spoken language development is more variable in implanted than normal hearing children, [35, 36] for reasons including pre-implantation sensory deprivation and asynchronous auditory restoration. Second, the children receiving CI span the critical period of language development, coupled with exposure to different languages (i.e., English, Spanish and Cantonese) that may be subserved by different brain networks. [37-39] Third, spoken language development is further influenced by differences in site-specific rehabilitation protocols and maternal education. Fourth, technical heterogeneity arises from variations in MRI scanners and protocols, surgical techniques, implant device types, and implant programming methods. Collectively, these compounding sources of variability establish a challenging real-world validation environment wherein conventional

neural predictive models often fail, thereby providing an ideal benchmark for evaluating the generalizability-critical features of our framework.

Results

The susceptibility of deep learning

We evaluated the applicability of deep transfer learning models across four distinct CI datasets under both in-domain and cross-domain settings to gain insights into their generalizability. Here, we first assessed the performance of models on various single datasets, including children in the Chicago area who were learning English (henceforth “Chicago English”) or Spanish (“Chicago Spanish”), children in the Melbourne area learning English (“Melbourne English”), children in Hong Kong learning Cantonese (“Hong Kong Cantonese”), as well as on their combined datasets: Chicago English + Chicago Spanish, Chicago English + Melbourne English, Chicago English + Chicago Spanish + Melbourne English, and Chicago English + Chicago Spanish + Melbourne English + Hong Kong Cantonese. Furthermore, we tested whether the model trained on the largest dataset (Chicago English) could predict outcomes for three specific cross-domain scenarios: 1) learning Spanish at the same center (Chicago Spanish), 2) learning the same language at another medical center (Melbourne English), and 3) learning a different language at a different center (Hong Kong Cantonese).

Regardless of whether a single dataset or a combination of different datasets was used to build the model, the transfer learning model demonstrated consistently accurate performance (Table S1 and Figure 1). It achieved an ACC of 87.59% (95% CI, 87.12%-88.05%) and AUC of 0.876 (95% CI, 0.872-0.88) across the Chicago and Melbourne datasets. When tested across the combined Chicago, Melbourne, and Hong Kong datasets, it achieved an ACC of 87.12% (95% CI, 86.05%-88.19%) and AUC of 0.871 (95% CI, 0.860-0.882). However, when the model was externally tested for generalization using data from another medical center (e.g., testing the Chicago English model with Melbourne English data), its performance dropped to chance levels (ACC: 50.95% (95% CI, 49.14%-53.75%)).

and AUC: 0.511 (95% CI, 0.489-0.533)). Even within the same center, cross-language generalization (e.g., testing the Chicago English model with Chicago Spanish data) could not be achieved with our sample sizes (ACC: 50.27% (95% CI, 47.62%-53.76%) and AUC: 0.499 (95% CI, 0.467-0.532)). When tested across different languages and centers (e.g., testing the Chicago English model with Hong Kong Cantonese data), the model showed an ACC of 50.75% (95% CI, 47.62%-53.87%) and AUC of 0.500 (95% CI, 0.496-0.504). These results indicate that deep transfer learning is highly sensitive to cross-domain population differences, including variations in center and language, and undergoes significant performance degradation when applied to new target domains.

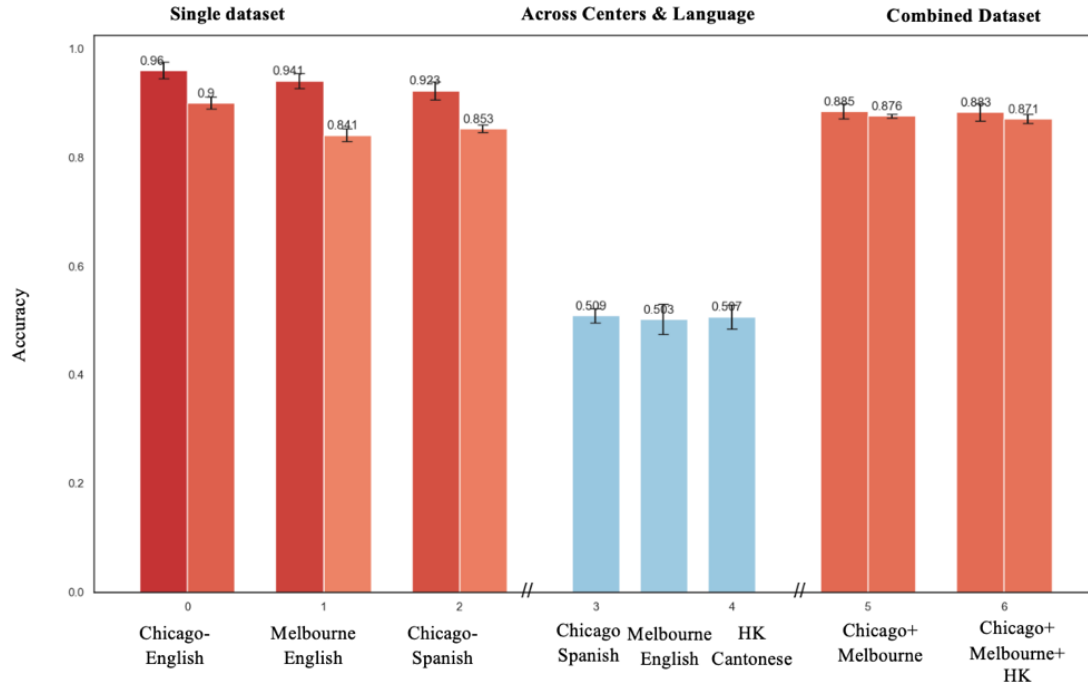


Figure 1. The internal and external evaluation performance for deep transfer learning.

The insufficient adaptability in domain adaptation

Domain adaptation methods aim to align joint distributions of source and target domains, allowing features from both domains to be projected into a shared space. However,

generalization in domain adaptation has often been treated as a pure representation learning problem, applying techniques to learn invariant feature representations across domains. These invariant features often fail to capture the nuances of OOD data or label shifts, as they are designed for cross-domain consistency rather than active adaptability. To demonstrate insufficient adaptability of domain adaptation, we assessed whether a transfer learning model with domain adaptation, trained on the largest dataset (Chicago English), could adapt to various OOD scenarios. Specifically, we examined how well the model adapted to CI candidates learning a different language at the same center (Chicago Spanish), learning the same language at a different center (Melbourne English), and learning a different language at a different center (HK Cantonese). These scenarios involved both feature shifts and label shifts, as children’s spoken language abilities were assessed using different tools across centers.

The performances of deep transfer learning with domain adaptation is summarized in Table S2. Cross-domain evaluation achieved an ACC of 43.81% (95% CI, 38.32%-49.31%) and AUC of 0.438 (95% CI, 0.383-0.493) in Melbourne-English dataset, ACC of 55.50% (95% CI, 43.52%-67.74%) and AUC of 0.556 (95% CI, 0.433-0.677) in Chicago-Spanish dataset, and ACC of 53.73% (95% CI, 34.43%-73.02%) and AUC of 0.545 (95% CI, 0.352-0.738) in Hong Kong-Cantenese dataset. The results suggest that domain adaptation methods rely heavily on static representation learning while lacking the flexibility to adapt to OOD environments, particularly during label shifts.

Uncertainty exploration in directed evolution algorithm

Generalization requires AI systems to apply prior experiences to unseen, novel conditions. While current RL algorithms excel at exploring optimal policies through strategies like value backups[40] and returns[41], they often neglect uncertainty exploration, which means these

strategies have difficulty exploring when uncertainty changes. The lack of uncertainty exploration strategy limits their ability to generalize to real-world environments. The trial-and-error approach of directed evolution is one of the most efficient exploration methods for developing new entities with desired traits. [42] By iteratively applying mutation, selection, and amplification, this approach rapidly explores a wide range of potential variations, enabling the identification of new solutions, even in complex or poorly understood systems (see Figure 2a). [43] Designing a computational model that mimics the trial-and-error process of directed evolution requires an AI system capable of optimizing the model through continuous screening across different subsets (selection) and evolving candidate features with pseudo-label variants (mutation) (see Figure 2b).

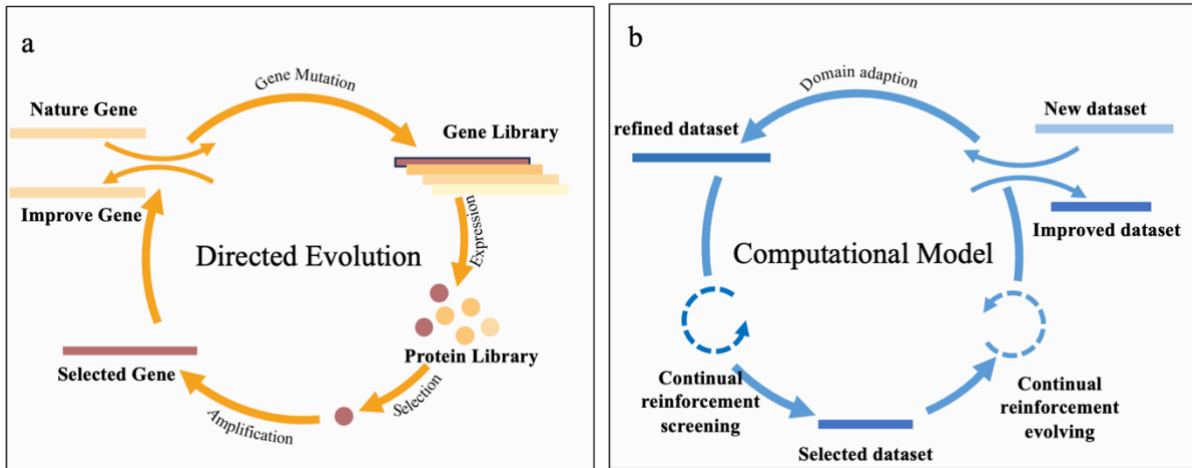


Figure 2. **a**, Directed evolution is a laboratory technique that expedites the natural evolution process by iteratively applying cycles of selection and mutation. **b**, Inspired by biological evolution, we propose DEM, an evolutionary computational model that composes iterative approaches into a continual reinforcement learning framework to address uncertainty exploration issues.

DEM includes two learning phases (see Figure 3d): First, the screening phase aims to identify high-confidence subsets via a confidence-calibrating mechanism that is more adaptable for domain shifts. This improves the cross-domain performance of neural prediction models. The resulting high-confidence pseudo-labels allow the model to work with unlabeled target data in a supervised manner [44-46]. Second, the evolving phase simulates the process of evolution (i.e., mutation and crossover), which enhances the diversity of candidate pseudo-labels and selects the fittest ones (see Figure 3b). Consequently, this evolutionary computation strategy allows DEM to guide the agent’s exploration behaviours, reducing uncertainty and enabling more targeted and rapid adaption.

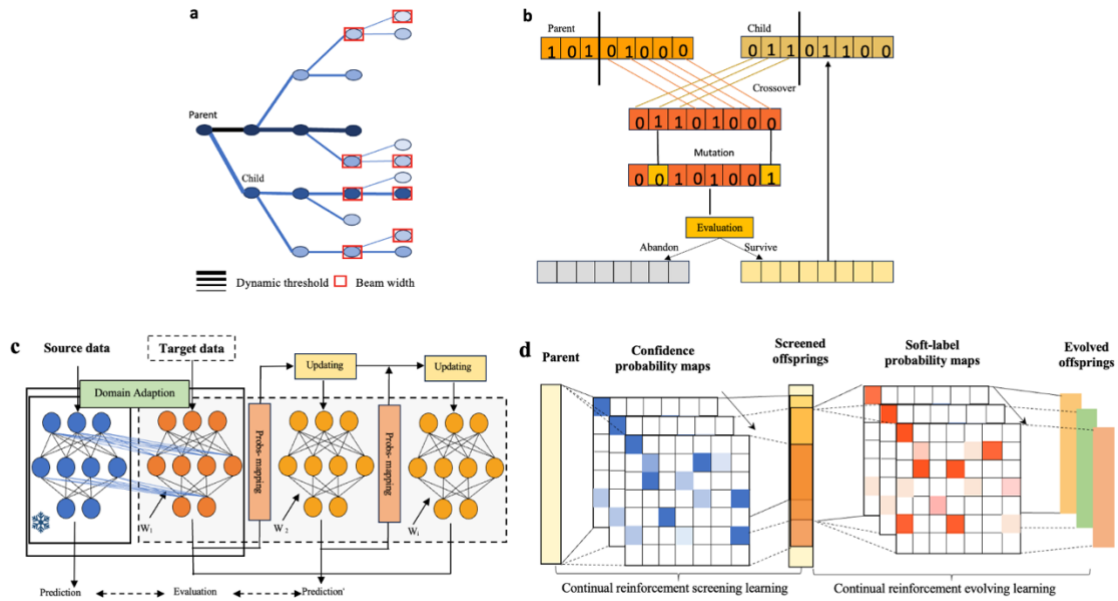


Figure 3. a, The beam search approach was adapted to the replay buffer in continual reinforcement learning, providing a more structured and prioritized mechanism for recalling useful past information. b, Mutation and crossover steps were modified and integrated with beam search to optimize candidate labels and models, enabling the selection of the best offspring labels. c, Unlike domain adaptation learning, we designed a dynamic dataset framework by sample selection and mutation strategies, simulating the agent-environment

interaction in uncertainty exploration in reinforcement learning (RL). This strategy learns and optimizes neural predictive models in an supervised manner, while catastrophic forgetting is mitigated by transferring knowledge from source to target domain through continual learning (CL) during each iteration. d, DEM combined CL and RL to coordinate multiple parallel learners using a confidence calibration mechanism, guiding both the screening and evolution phases.

Generalization in DEM

We evaluated the generalizability of DEM in cross-domain neural prediction in which the training (Chicago English) and testing data exhibit distinct distributions in terms of center and/or language: Chicago Spanish (same center, different language), Melbourne English (different center, same language), and Hong Kong Cantonese (different center, different language). Following the general setting of domain adaptation, we use all labeled source domain data and 80% unlabeled target domain data as the training set, and the remaining 20% labeled target domain data as the testing set. [47] To adapt labeled source domain to the unlabelled target domain, we first pretrained a source-led model in which labelled source training data and unlabelled target data were inputs. Performance was then measured on the source testing dataset. Source-pretrained parameters were frozen for the downstream continual reinforcement training loop. Next, we utilized a pretrained model to acquire target predictions as the initial pseudo-labeled target samples. Finally, high-confidence samples and pseudo-label variants were iteratively produced from screening and evolving processes, respectively. Therefore, the continual reinforcement neural network was iteratively trained on selective samples (screening phase) and refined pseudo-labels (evolving phase), after which its performance was measured on the target testing dataset.

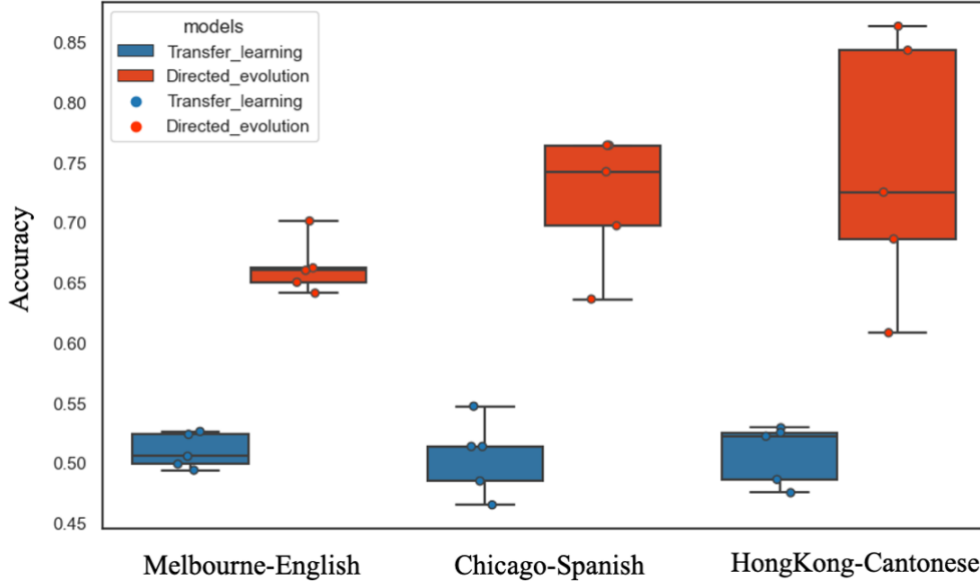


Figure 4. Cross-domain performance comparison between transfer learning and DEM on three new datasets. The box plots display the mean five-fold cross-validation accuracy of cross-domain evaluations on the target data. The transfer learning model is trained on source data and directly evaluated on target data, while DEM is trained on source data and evaluated on target test data after applying directed evolution learning to the unlabelled target training data.

The cross-domain performance on Chicago Spanish, Melbourne English, and Hong Kong Cantonese is presented in Figure 4 and Table S4. DEM exhibited significantly superior performance compared to the transfer learning model. Specifically, it outperformed the transfer learning model by 22% (Chicago Spanish), 17% (Melbourne English), and 35% (Hong Kong Cantonese) in accuracy (ACC). These results show that the DEM is efficient and robust across various cross-domain settings, including different centers and languages. Furthermore, the findings provide evidence of cross-center and cross-language generalization even when training labels in the target domain are unavailable, which improves the effectiveness of DEM in real-world scenarios.

The explainability of DEM

We conducted a series of ablation experiments to enhance the explainability of DEM. The results are presented in Table S5-7 and Figure 5. We first evaluated the effectiveness of the continual reinforcement learning (CRL) framework. This involved examining whether a model trained on source data could be effectively applied to a series of unseen and evolving target datasets, while still preserving previously learned knowledge from the source domain during transition to these dynamic target tasks. Three network variations were investigated: RL, CRL without domain adaptation, CRL with domain adaptation. As shown in Table S5 and Figure 5a, both CRL networks outperform RL in cross-domain evaluations, indicating that the combined framework enhances exploration and generalization. In contrast, domain-specific RL framework lacks mutual information and tends to amplify errors in the pseudo-labeling strategy derived solely from source data, resulting in a restricted learning scope. Additionally, CRL with domain adaptation demonstrates superior performance compared to CRL without domain adaptation. By incorporating domain adaptation, the framework actively aligns source and target feature spaces during each action, reducing domain-specific biases and improving the model's generalization to target data. The findings highlight that RL is susceptible to dramatic overfitting within predefined training environments. In contrast, adaptive continual learning (CL) ensures dynamic mutual information transfer while retaining foundational knowledge from source-domain pretraining. Consequently, by leveraging the synergy between these approaches, CRL enables the model to balance rapid optimization for dynamic target tasks while preserving knowledge from the source domain.

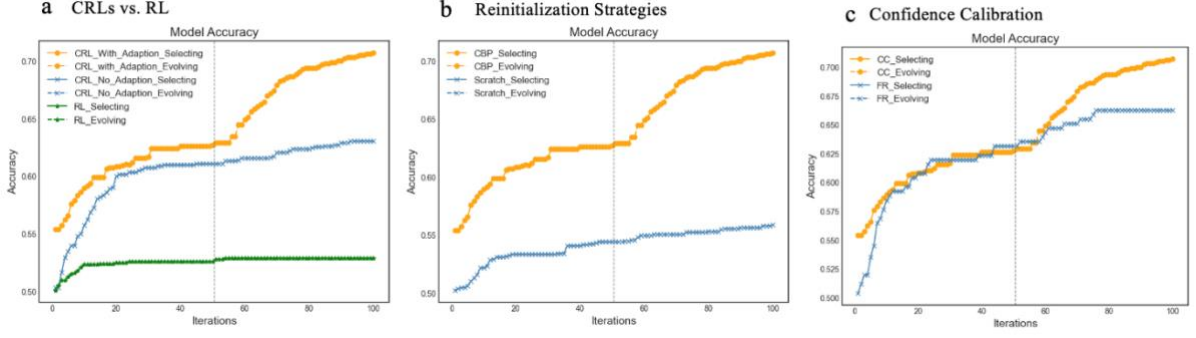


Figure 5. Ablation study results: analyzing the impact of key components on DEM’s selecting and evolving stages. a, In model framework comparisons, RL represents a domain-specific framework that relies on domain-specific data during both pretraining (source dataset) and continuous training (target datasets). CRL_No_Adaption represents a CRL without domain adaptation and DEM represents CRL with domain adaptation. b, In terms of reinitialization strategies, scratch refers to a training model from initialized model state and CBP refers to a framework utilizing continual backpropagate strategy that can mitigate the occurrence of "dead" units during continuous training. c, Regarding confidence calibration strategies, RF represents a model utilizing a fixed confidence filtering mechanism for selecting stage and a random mutation mechanism for evolving stage and CC represents a DEM model utilizing a proposed confidence calibration mechanism for both the selecting and evolving stages.

To assess the effectiveness of replay buffer and continual backpropagate strategies in balancing exploration and exploitation in CRL, we compared CRL training from scratch with CRL using continual reinitialization. That is, if CRL with reinitialization performs better than the network training from scratch, there is a benefit owing to training on previous classes that indicate our cycling network is an incrementally trained network, and if it performs worse, then there is forgetting or loss of plasticity. The results showed that CRL with continual

reinitialization exhibited better performance than CRL training from scratch (see Table S6 and Figure 5b), underscoring the importance of maintaining plasticity in deep RL systems. Altogether, these findings indicated CRL equipped with replay buffer and continual backpropagate strategies can provide a better compromise between plasticity and stability, and coordinate multiple continual learners to ensure solution compatibility.

To validate the effectiveness of confidence calibration in screening and evolving processes, we evaluated the model with a fixed threshold mechanism in the screening phase and a random mutation mechanism in the evolving phase. Performance was compared with DEM using a confidence calibration mechanism. We found the confidence calibration mechanism improved the performance by 5% in ACC (Table S7 and Figure 5c). Moreover, evolving learning increased the probability of exploring potentially better options at a lower computational cost, as demonstrated by an improvement of 8% in ACC following the screening phase. These results indicate that proposed confidence calibration can efficiently enhance overall performance compared to random methods, while also providing interpretable insights for the prediction results.

Discussion

Domain shift and label scarcity leave hospitals and medical AI tools in a challenging position, especially as some medical institutions experiment with ways to use and evaluate AI algorithms in medicine [4, 10, 23]. In this study, we developed DEM, a novel directed evolution algorithm to tackle these challenges, applying it to forecast spoken language improvement. The results show that DEM can adapt to different centers and language environments, in addition to variability inherent to the child, to forecast spoken language improvements over a period of up to three years for children who will receive a CI. Moreover, ablation experiments reveal how different components of our model contribute to the final performance, highlighting its significant potential for adapting to new, unseen environments. By incorporating directed evolution into the CRL framework, we demonstrated DEM's capacity for uncertainty exploration by driving the agent towards promising states without the need for exhaustive exploration.

Developing a universal model on a large, representative multi-center dataset that generalizes to unseen datasets is highly desirable. In practice, however, it is hard to acquire fully annotated data and difficult to allow data sharing across centers. Domain shift in medical datasets further complicates clinical applications. As a result, models that performed well in one dataset routinely failed to generalize to unseen patients. [1] Therefore, developing high-quality machine learning algorithms that can capture useful information across centers is essential for achieving more generalisable models. [4, 48] DEM can provide a rapid domain adaptation approach that can improve reliability in the face of challenges including domain shift and label scarcity. By leveraging evolutionary strategies, DEM creates a agent/environment interaction for neural prediction in the medical field. Pseudo-labelling strategies were incorporated to address label scarcity, allowing the model to deploy to different population groups, especially where labelled data is expensive and sparse.

Uncertainty exploration strategies are crucial for improving generalization in RL. [29, 49] By shifting from static representation learning to active exploration learning, directed evolution algorithm efficiently guides the uncertainty exploration process, enhancing model generalization in RL. This means that DEM as a proactive problem-solving framework can continuously adapt to change and adjust its actions accordingly in an evolutionary computation manner. Grounded in directed evolution theory, this bio-inspired algorithm exhibits a solid theoretical foundation and high explainability. The exceptional OOD robustness and rapid domain adaptability will enable this promising approach to be extended and used across a variety of fields, including but not limited to neural prediction, precision education, drug development, and autonomous systems.

Methods

DEM structure

Combining CL and RL is essential for establishing an effective intelligent learning system that optimizes the DEM model through iterative selection and evolution strategies. CL can empower the model with strong adaptability to continuously learn new knowledge and avoid catastrophic forgetting [50]. RL, with its trial-and-error nature, introduces additional complexities by requiring the capacity of identification depending on context and exploration outcomes and balancing the exploitation of known effective states with the exploration of new possibilities.[51, 52] By combining RL's optimization with CL's adaptability, CRL enables the model to effectively balance exploitation and exploration in new and dynamic target tasks while preserving knowledge from the known source domain (see Figure 3c). Notably, catastrophic forgetting in CL differs fundamentally from episodic forgetting in RL. In CL, tasks are typically more structured and sequential, requiring the model to retain

knowledge of previously learned tasks while accommodating new ones. In contrast, RL operates in dynamic and uncertain environments, where the focus is not on avoiding the forgetting of specific tasks but on balancing the retention of effective past experiences with the exploration of potentially better options. While both CL and RL share a focus on maintaining memory stability, CL focus on preserving past knowledge, whereas RL requires strategic exploration to find the best solution quickly, rather than solely relying on memorization. In this context, CRL plays a pivotal role in bridging the gap between the source domain and dynamic target environments, facilitating knowledge transfer while ensuring adaptability and stability in ever-changing settings.

As for CL framework, we adopted a progressive CL with domain adaptation, called adaptive CL, to mitigate the mutual interference between source and target domain. Adaptive CL incorporated progressive CL with a joint domain adaptation optimization algorithm (see supplementary materials) to learn invariant representations across domain while avoiding catastrophic forgetting [24]. This module starts with both source-column and target-column networks. The optimization of parameters is first trained to convergence on the source data. When transitioning to the target data, the parameters of source-column were frozen, and the parameters of target-column were retrained to adapt to a set of target datasets. Thus, during CRL training for different target candidates from the screening and evolving learning phases, all target-column parameters are kept close to the frozen source-column parameters, facilitating knowledge transfer from source to target domain.

As for RL framework, we integrated evolutionary learning strategies into the RL framework to simulate the feedback mechanism which is essential for continuous improvement and adaptation needed for medical applications. To avoid random or ϵ -greedy exploration in an uncertain environment where not all states are informative, we implemented a novel uncertainty exploration strategy inspired by directed evolution algorithm. It incorporated

evolutionary computation strategies, such as sample selection and mutation with beam search strategy, to identify and prioritize the most informative states during iterative learning and continuously improve the model's adaptability to a new environment. [53-55]

Specifically, we first introduced a pseudo-label strategy based on an pretrained source-led model into both selecting and evolving stages to address the issue of label scarcity in the target domain. Then, we iteratively trained the classifier model on a subset of target samples with pseudo labels during screening learning, where each sample subset (selection pattern) is selected based on log-probabilities derived from a Bernoulli distribution parameterized by probabilities from the policy model. Here, we treated the entire selection pattern as a single action with a joint probability that is the sum of log probabilities of each selection. So RL learning can be formulated as follows:

$$J_{sel}P(a) = \sum_{i=1}^K \log P(S_i)$$

Where $J_{sel}P(a)$ is the joint probability of the entire selection pattern as one action; $P(S_i)$ is the probability of the i -th selection.

Next, candidate pseudo labels were also updated by joint log-probabilities of Bernoulli distribution parameterized by probabilities from the policy model during evolving learning to enhance the diversity of candidate pseudo labels.

$$J_{mut}P(a) = \sum_{i=1}^K \log P(L_i)$$

Where $J_{mut}P(a)$ is the joint probability of the entire mutation pattern as one action; $P(L_i)$ is the probability of the i -th mutation (labels).

Additionally, due to the confidence bias, we implemented a confidence-calibration mechanism to alleviate the mis-labeling issue during training, which is discussed later. In the context of evolutionary RL framework, the reward was based on the performance of a classifier trained on the dataset selected by action. While the model might struggle to directly attribute the reward to specific samples, the joint probability ensures that the policy can iteratively refine the probability of selection patterns that improve model performance. To improve the diversity of model exploration, we implemented entropy regularization to the loss. Moreover, we utilized a patience mechanism in the beam search process for both selecting and evolving learning to avoid inefficient exploration that can break out of loops when the updated accuracy is not increasing after a specified number of consecutive times. After several iterations of learning, we collected a batch of N actions to compute the total loss as follows:

$$L = \frac{1}{N} \sum_{n=1}^N (-\log P(a_n) \cdot R_n - \beta H(a_n))$$

Where $P(a_n)$ is the probability of the action a_n , and R_n is its reward, β is a coefficient that controls the weight of the entropy term, and $H(a_n)$ is the entropy of the policy for action a_n . We define $H(a_n)$ as:

$$H(a_n) = - \sum_{i=1}^{K_n} [p_{n,i} \log p_{n,i} + (1 - p_{n,i}) \log (1 - p_{n,i})]$$

Where each action a_n consists of K_n independent binary components (e.g., sample selection or label mutation), and $p_{n,i}$ represents the Bernoulli probability for the i component.

The aim of DEM learning is to improve the efficiency of uncertainty exploration in RL by utilizing the rule of biological evolution derived from directed evolution. Evolution computation strategies guide uncertainty exploration of iterative learnings within RL through breaking through the previous sequential RL learning mode and effectively implementing the

cycling of screening and evolving learning. Consequently, the RL policy was updated based on feedback from iterations of evolutionary learning so that the agent adjusts its parameters to improve the performance of subsequent training. Therefore, evolutionary RL, an ensemble-like training approach, can efficiently balance immediate reward in evolutionary learning with long-term reward optimization in RL.

The balance between exploitation and exploration

A key challenge in RL is maintaining the balance between exploitation and exploration. Although exploration strategy is crucial for improving generalization in reinforcement learning, most of approaches are limited by insufficient exploration and the unophisticated exploration strategies. Striking a balance between exploitation and exploration not only improves performance within training environments but also helps the model acquire the knowledge needed to generalize to new, unseen situations. Here we leveraged an experience replay algorithm to iteratively revisit and learn from the most informative experiences in the past (stability). [56] Specifically, we incorporated beam search strategy into relay buffer to store and prioritize old experiences based on their importance (see Figure 3a). On the other hand, continual backpropagate strategy was integrated to efficiently explore new useful information (plasticity) within CRL that can reinitialize a small fraction of less-used and death units. [52] Moreover, replay buffer is different but complementary to continual backpropagate as it can break the sequential experiences through iteratively replaying promising states and avoid the agent stuck in poor states.

Confidence calibration mechanism

The traditional selection and evolution processes at random are the easiest methods, but are time- and labour-intensive. Here, we introduced a novel confidence calibration strategy for CRL that enhances the efficiency of both screening and evolving processes by selecting

better candidates based on calibrated confidences. This mechanism incorporates both memory forgetting and memory protection to ensure a smooth transition between new and old data and prevent a drastic or incompatible change. [57]

The confidence calibration approach is inspired by the protecting and forgetting mechanism to ensure the accumulation of incremental changes by calibrating confidences of predictions in every iteration. This means a high and calibrated confidences of predictions will be selected by the protecting and forgetting mechanism based on the feedback from each subset. The protecting term preserves successful search by keeping confidences close to their values from the previous iteration. The forgetting term allows the algorithm to adjusting confidences back toward their initial values, ensuring that bad searches can be ‘forgotten’ and better ones can be explored. We can formulize this regulation methods as follows:

$$C_{I_j}^{updated} = C_j^{prev} + \underbrace{\lambda \left(C_j^{curr} - C_{I_j}^{prev} \right)^2}_{\text{protecting term}} - \underbrace{(1 - \lambda) \left(C_j^{prev} - C_{I_j}^{init} \right)^2}_{\text{forgetting term}}$$

Where $C_j^{curr} \in \mathbb{R}^M$ denotes as the confidence of the sample at index I_j in the sub-dataset, with M samples, $C_{I_j}^{prev} \in \mathbb{R}^Z$ denotes as the confidence of the sample at index I_j in the previous iteration for Z samples, $C_{I_j}^{init}$ is the initial confidence of all N samples at index I_j in the dataset, $I \in \mathbb{Z}^K$ denotes as the indices of the K samples in the subdataset, referring to their positions in the full dataset of size N , and λ is a hyperparameter that dominate improvement or degradation in performance. Here we define

$$\lambda = \frac{1}{1 + \exp(-k \cdot \Delta_{acc})}$$

Where k is a scaling factor that controls the steepness of the transition and Δ_{acc} is the accuracy change.

Acknowledgements

This work was supported by the Research Grants Council of Hong Kong Grant GRF14605119, National Institutes of Health R21DC016069 and R01DC019387.

Ethics Declarations

Nancy M. Young has received research funding from MEDEL for an FDA clinical trial unrelated to this study. Patrick C. M. Wong is the founder of a startup company supported by funds from the Hong Kong SAR Government, which is also unrelated to this study. Yanlin Wang and Patrick Wong declare that a US provisional patent application in relation to DEM as a process (but not specifically to its application to children with CI) has been filed (080015-1494452-042600US). No other declarations were reported.

Reference:

- [1] A. M. Chekroud *et al.*, "Illusory generalizability of clinical prediction models," *Science*, vol. 383, no. 6679, pp. 164-167, 2024, doi: doi:10.1126/science.adg8538.
- [2] R. A. Poldrack, G. Huckins, and G. Varoquaux, "Establishment of best practices for evidence for prediction: a review," *JAMA psychiatry*, vol. 77, no. 5, pp. 534-540, 2020.
- [3] J. Wu, J. Li, S. B. Eickhoff, D. Scheinost, and S. Genon, "The challenges and prospects of brain-based prediction of behaviour," *Nature Human Behaviour*, vol. 7, no. 8, pp. 1255-1264, 2023/08/01 2023, doi: 10.1038/s41562-023-01670-1.
- [4] M. Lenharo, "The testing of AI in medicine is a mess. Here's how it should be done," *Nature*, vol. 632, no. 8026, pp. 722-724, 2024.
- [5] J. Ash and R. P. Adams, "On warm-starting neural network training," *Advances in neural information processing systems*, vol. 33, pp. 3884-3894, 2020.
- [6] P. Hager *et al.*, "Evaluation and mitigation of the limitations of large language models in clinical decision-making," *Nature Medicine*, vol. 30, no. 9, pp. 2613-2622, 2024/09/01 2024, doi: 10.1038/s41591-024-03097-1.
- [7] P. Rajpurkar, E. Chen, O. Banerjee, and E. J. Topol, "AI in health and medicine," *Nature medicine*, vol. 28, no. 1, pp. 31-38, 2022.
- [8] M. Moor *et al.*, "Foundation models for generalist medical artificial intelligence," *Nature*, vol. 616, no. 7956, pp. 259-265, 2023.
- [9] L. Goetz, N. Seedat, R. Vandersluis, and M. van der Schaar, "Generalization—a key challenge for responsible AI in patient-facing clinical applications," *npj Digital Medicine*, vol. 7, no. 1, p. 126, 2024.
- [10] D. C. Castro, I. Walker, and B. Glocker, "Causality matters in medical imaging," *Nature Communications*, vol. 11, no. 1, p. 3673, 2020/07/22 2020, doi: 10.1038/s41467-020-17478-w.
- [11] G. Yu *et al.*, "Accurate recognition of colorectal cancer with semi-supervised deep learning on pathological images," *Nature Communications*, vol. 12, no. 1, p. 6311, 2021/11/02 2021, doi: 10.1038/s41467-021-26643-8.
- [12] H. Guan and M. Liu, "Domain Adaptation for Medical Image Analysis: A Survey," (in eng), *IEEE Trans Biomed Eng*, vol. 69, no. 3, pp. 1173-1185, Mar 2022, doi: 10.1109/tbme.2021.3117407.
- [13] R. A. I. Bethlehem *et al.*, "Brain charts for the human lifespan," *Nature*, vol. 604, no. 7906, pp. 525-533, 2022/04/01 2022, doi: 10.1038/s41586-022-04554-y.
- [14] E. Courchesne *et al.*, "Mapping early brain development in autism," (in eng), *Neuron*, vol. 56, no. 2, pp. 399-413, Oct 25 2007, doi: 10.1016/j.neuron.2007.10.016.
- [15] O. Russakovsky *et al.*, "Imagenet large scale visual recognition challenge," *International journal of computer vision*, vol. 115, pp. 211-252, 2015.
- [16] J. Achiam *et al.*, "Gpt-4 technical report," *arXiv preprint arXiv:2303.08774*, 2023.
- [17] J. Wang *et al.*, "Generalizing to unseen domains: A survey on domain generalization," *IEEE transactions on knowledge and data engineering*, vol. 35, no. 8, pp. 8052-8072, 2022.
- [18] C. Tan, F. Sun, T. Kong, W. Zhang, C. Yang, and C. Liu, "A survey on deep transfer learning," in *Artificial Neural Networks and Machine Learning–ICANN 2018: 27th International Conference on Artificial Neural Networks, Rhodes, Greece, October 4–7, 2018, Proceedings, Part III* 27, 2018: Springer, pp. 270-279.
- [19] A. P. Azad, M. Padmanaban, and V. Arya, "A data lens into MPPT efficiency and PV power prediction," in *2018 IEEE Power & Energy Society Innovative Smart Grid Technologies Conference (ISGT)*, 2018: IEEE, pp. 1-5.

- [20] Y. Ganin *et al.*, "Domain-adversarial training of neural networks," *Journal of machine learning research*, vol. 17, no. 59, pp. 1-35, 2016.
- [21] W. M. Kouw and M. Loog, "A review of domain adaptation without target labels," *IEEE transactions on pattern analysis and machine intelligence*, vol. 43, no. 3, pp. 766-785, 2019.
- [22] C. Packer, K. Gao, J. Kos, P. Krähenbühl, V. Koltun, and D. Song, "Assessing generalization in deep reinforcement learning," *arXiv preprint arXiv:1810.12282*, 2018.
- [23] J. Futoma, M. Simons, T. Panch, F. Doshi-Velez, and L. A. Celi, "The myth of generalisability in clinical research and machine learning in health care," *The Lancet Digital Health*, vol. 2, no. 9, pp. e489-e492, 2020, doi: 10.1016/S2589-7500(20)30186-2.
- [24] G. I. Parisi, R. Kemker, J. L. Part, C. Kanan, and S. Wermter, "Continual lifelong learning with neural networks: A review," *Neural networks*, vol. 113, pp. 54-71, 2019.
- [25] C. S. Lee and A. Y. Lee, "Clinical applications of continual learning machine learning," *The Lancet Digital Health*, vol. 2, no. 6, pp. e279-e281, 2020.
- [26] N. Jones, "'In awe': scientists impressed by latest ChatGPT model o1," (in eng), *Nature*, vol. 634, no. 8033, pp. 275-276, Oct 2024, doi: 10.1038/d41586-024-03169-9.
- [27] R. S. Sutton, "Introduction to reinforcement learning with function approximation," in *Tutorial at the conference on neural information processing systems*, 2015, vol. 33.
- [28] M. E. Taylor and P. Stone, "Transfer learning for reinforcement learning domains: A survey," *Journal of Machine Learning Research*, vol. 10, no. 7, 2009.
- [29] Y. Jiang, J. Z. Kolter, and R. Raileanu, "On the importance of exploration for generalization in reinforcement learning," *Advances in Neural Information Processing Systems*, vol. 36, 2024.
- [30] J. Cockburn, V. Man, W. A. Cunningham, and J. P. O'Doherty, "Novelty and uncertainty regulate the balance between exploration and exploitation through distinct mechanisms in the human brain," *Neuron*, vol. 110, no. 16, pp. 2691-2702. e8, 2022.
- [31] F. H. Arnold, "Design by directed evolution," *Accounts of chemical research*, vol. 31, no. 3, pp. 125-131, 1998.
- [32] F. H. Arnold, "Directed evolution: bringing new chemistry to life," *Angewandte Chemie (International Ed. in English)*, vol. 57, no. 16, p. 4143, 2017.
- [33] R. Miikkulainen and S. Forrest, "A biological perspective on evolutionary computation," *Nature Machine Intelligence*, vol. 3, no. 1, pp. 9-15, 2021.
- [34] M. C. Flickinger and S. W. Drew, "FERMENTATION, BIOCATALYSIS," 1999.
- [35] G. Feng *et al.*, "Neural preservation underlies speech improvement from auditory deprivation in young cochlear implant recipients," *Proceedings of the National Academy of Sciences*, vol. 115, no. 5, pp. E1022-E1031, 2018.
- [36] D. Yuan *et al.*, "Predicting Auditory Skill Outcomes After Pediatric Cochlear Implantation Using Preoperative Brain Imaging," *American Journal of Audiology*, vol. 34, no. 1, pp. 51-59, 2025.
- [37] E. Bialystok, "The bilingual adaptation: How minds accommodate experience," (in eng), *Psychol Bull*, vol. 143, no. 3, pp. 233-262, Mar 2017, doi: 10.1037/bul0000099.
- [38] J. Ge *et al.*, "Cross-language differences in the brain network subserving intelligible speech," (in eng), *Proc Natl Acad Sci U S A*, vol. 112, no. 10, pp. 2972-7, Mar 10 2015, doi: 10.1073/pnas.1416000112.
- [39] J. K. Niparko *et al.*, "Spoken language development in children following cochlear implantation," *Jama*, vol. 303, no. 15, pp. 1498-1506, 2010.

- [40] V. Mnih *et al.*, "Human-level control through deep reinforcement learning," *Nature*, vol. 518, no. 7540, pp. 529-533, 2015/02/01 2015, doi: 10.1038/nature14236.
- [41] J. Schulman, F. Wolski, P. Dhariwal, A. Radford, and O. Klimov, "Proximal policy optimization algorithms," *arXiv preprint arXiv:1707.06347*, 2017.
- [42] E. T. Boder, K. S. Midelfort, and K. D. Wittrup, "Directed evolution of antibody fragments with monovalent femtomolar antigen-binding affinity," *Proceedings of the National Academy of Sciences*, vol. 97, no. 20, pp. 10701-10705, 2000.
- [43] Y. Yokobayashi, R. Weiss, and F. H. Arnold, "Directed evolution of a genetic circuit," *Proceedings of the National Academy of Sciences*, vol. 99, no. 26, pp. 16587-16591, 2002.
- [44] D.-H. Lee, "Pseudo-label: The simple and efficient semi-supervised learning method for deep neural networks," in *Workshop on challenges in representation learning, ICML, 2013*, vol. 3, no. 2: Atlanta, p. 896.
- [45] E. Arazo, D. Ortego, P. Albert, N. E. O'Connor, and K. McGuinness, "Pseudo-labeling and confirmation bias in deep semi-supervised learning," in *2020 International joint conference on neural networks (IJCNN)*, 2020: IEEE, pp. 1-8.
- [46] P. Cascante-Bonilla, F. Tan, Y. Qi, and V. Ordonez, "Curriculum labeling: Revisiting pseudo-labeling for semi-supervised learning," in *Proceedings of the AAAI conference on artificial intelligence*, 2021, vol. 35, no. 8, pp. 6912-6920.
- [47] P. Bai, F. Miljković, B. John, and H. Lu, "Interpretable bilinear attention network with domain adaptation improves drug–target prediction," *Nature Machine Intelligence*, vol. 5, no. 2, pp. 126-136, 2023.
- [48] J. Futoma, M. Simons, T. Panch, F. Doshi-Velez, and L. A. Celi, "The myth of generalisability in clinical research and machine learning in health care," (in eng), *Lancet Digit Health*, vol. 2, no. 9, pp. e489-e492, Sep 2020, doi: 10.1016/s2589-7500(20)30186-2.
- [49] P. Ladosz, L. Weng, M. Kim, and H. Oh, "Exploration in deep reinforcement learning: A survey," *Information Fusion*, vol. 85, pp. 1-22, 2022.
- [50] J. Kirkpatrick *et al.*, "Overcoming catastrophic forgetting in neural networks," *Proceedings of the national academy of sciences*, vol. 114, no. 13, pp. 3521-3526, 2017.
- [51] M. L. Littman, "Reinforcement learning improves behaviour from evaluative feedback," *Nature*, vol. 521, no. 7553, pp. 445-451, 2015.
- [52] S. Dohare, J. F. Hernandez-Garcia, Q. Lan, P. Rahman, A. R. Mahmood, and R. S. Sutton, "Loss of plasticity in deep continual learning," *Nature*, vol. 632, no. 8026, pp. 768-774, 2024.
- [53] Y. Wang *et al.*, "Continual test-time domain adaptation via dynamic sample selection," in *Proceedings of the IEEE/CVF Winter Conference on Applications of Computer Vision*, 2024, pp. 1701-1710.
- [54] D. A. Bennett *et al.*, "Prevalence of parkinsonian signs and associated mortality in a community population of older people," *New England Journal of Medicine*, vol. 334, no. 2, pp. 71-76, 1996.
- [55] Z. D. Guo and E. Brunskill, "Directed exploration for reinforcement learning," *arXiv preprint arXiv:1906.07805*, 2019.
- [56] T. Schaul, "Prioritized Experience Replay," *arXiv preprint arXiv:1511.05952*, 2015.
- [57] L. Wang *et al.*, "Incorporating neuro-inspired adaptability for continual learning in artificial intelligence," *Nature Machine Intelligence*, vol. 5, no. 12, pp. 1356-1368, 2023.

Supplementary Materials for

Directed evolution algorithm drives neural prediction

Yanlin Wang, Nancy M Young, Patrick C M Wong

Corresponding Authors: Patrick C M Wong, p.wong@cuhk.edu.hk

Datasets and Participants

This study analyzed data from 278 children with cochlear implants (CI), enrolled between 2009 and 2022 from three independent centers: Ann & Robert H. Lurie Children's Hospital of Chicago, Royal Victorian Eye and Ear Hospital (RVEEH), East Melbourne, Victoria, and Prince of Wales Hospital, Hong Kong SAR. These centers represented three languages: English (Chicago and Melbourne), Spanish (Melbourne), and Cantonese (Hong Kong). Specifically, 143 from Chicago English (67 female), 37 from Chicago Spanish (21 female), 81 from Melbourne (21 female), and 17 from Hong Kong (12 female). The mean age at sensorineural hearing loss (SNHL) diagnosis was 10.2 months (SD = 13.3) for Chicago, 11.1 months (SD = 12.4) for Melbourne, and 11.6 months (SD = 15.2) for Hong Kong; and the mean age at CI was 27.4 months (SD = 20.9) for Chicago, 30.1 months (SD = 18.4) for Melbourne, and 32.5 months (SD = 16.6) for Hong Kong.

Ethical Considerations and Exclusion Criteria

Children with conditions known to significantly impair language development or gross brain malformations were excluded from the study. Pre-implantation evaluations included T1-weighted structural whole-brain MRI, and their speech and language abilities were assessed both before and after implantation. Written informed consent was obtained from parents or guardians for access to the MRI scans and clinical data. Ethical approval was

secured from the Joint Chinese University of Hong Kong–New Territories East Cluster Clinical Research Ethics Committee, the Stanley Manne Children’s Research Institute’s Institutional Review Board, and The Royal Children’s Hospital Human Research Ethics Committee.

Spoken language measurements

Spoken language development was assessed differently across the three centers using age-appropriate tools. In Chicago, the Speech Recognition Index-modified version (SRI-m) was used before implantation and at multiple time points up to 36 months post-implantation. The SRI-m, a hierarchical battery of tests adapted to children’s age, development, and hearing abilities, provided scores rescaled to a 0–600 range, with higher scores indicating better spoken language abilities. In Melbourne, receptive and expressive language abilities were assessed using the Picture Peabody Vocabulary Test-4 (PPVT-4)[1] and Preschool Language Scale (PLS-4&5)[2] before implantation and at 12, 24, and 36 months post-implantation, offering standard scores with a mean of 100 and SD of 15. In Hong Kong, the LittleEARS Auditory Questionnaire, a 35-item caregiver-based assessment validated for children with normal hearing and hearing loss[3, 4], was used before implantation and at 6, 12, and 24 months post-implantation.

To quantify spoken language improvement over time, a linear mixed-effects model was constructed for each center with spoken language scores as the dependent variable, incorporating random intercepts for subject ID and random slopes for assessment time. Improvement was further classified into binary categories (high-improvement vs. low-improvement) using a median split within each center for enhanced model generalization.

MRI acquisition and preprocessing

T1-weighted MRI images were obtained from all participants prior to cochlear implantation (CI) across the three centers using various scanners and sequences optimized for high signal-to-noise ratios. The images were processed using the Advanced Normalization Tools (ANTs) in Python[5], resampled to a voxel size of 1 mm³, and preprocessed following standard T1-weighted MRI protocols. Deformation-based morphometry (DBM) was employed to identify whole-brain morphological differences[6]. From the DBM scans, 15 central axial 2D slices were extracted, cropped, and resized to 128×128 voxels. These slices were normalized using ImageNet statistics and assigned subject-specific labels for use as data samples in model training. Detailed scanning parameters for the MRI acquisition are as follows:

In Chicago, scans were performed on 3T Siemens scanners (MAGNETOM Skyra, Vida) using magnetization-prepared rapid gradient-echo (MPRAGE) sequences or on 3T General Electric scanners (DISCOVERY MR750, SIGNA Architect) using 3D brain volume (BRAVO) or Fast Spoiled Gradient Recalled Echo (FSPGR) sequences. Scanning parameters for BRAVO (N=43) were TE = 2.72–3.91 ms, TR = 7.40–9.45 ms, flip angle = 12°, matrix = 512×512, 148–512 slices, slice thickness = 1–2 mm, and voxel size = 0.3×0.3×0.6 mm to 0.5×0.5×1.4 mm. For FSPGR (N=1), parameters were TE = 4.3 ms, TR = 10.63 ms, flip angle = 20°, matrix = 256×256, 101 slices, slice thickness = 1.4 mm, and voxel size = 0.9×0.9×1.4 mm. For MPRAGE (N=136), parameters included TE = 2.38–3.54 ms, TR = 1490–2200 ms, flip angle = 8–9°, matrix = 192×192 to 512×512, 108–224 slices, slice thickness = 0.8–1 mm, and voxel size = 0.8×0.8×0.8 mm to 1×1×1 mm.

In Melbourne, scans were acquired using 1.5T Siemens scanners (MAGNETOM Area, Avanto, and SymphonyTim) and 3T Siemens scanners (MAGNETOM Trio and Verio) with MPRAGE sequences. Parameters (N=81) included TE = 2.31–4.92 ms, TR = 11–2100

ms, flip angle = 9° – 20° , matrix = 576×426 to 224×198 , 142–452 slices, slice thickness = 0.38–0.9 mm, and voxel size = $0.4 \times 0.4 \times 0.8$ mm to $0.9 \times 0.9 \times 0.9$ mm.

In Hong Kong, scans were conducted using 3T Siemens Prisma, General Electric, or Philips Achieva scanners with MPRAGE, BRAVO, or Turbo Field Echo (TFE) sequences. Parameters for the Siemens Prisma scanner were TE = 2.35–2.59 ms, TR = 1800 ms, flip angle = 8° , matrix = 256×208 to 640×640 , 192–320 slices, and slice thickness = 0.69–3 mm. For the General Electric scanner, parameters were TE = 2.68–2.81 ms, TR = 7.62–7.71 ms, flip angle = 12° , matrix = 512×512 , 146–352 slices, and slice thickness = 1–1.1 mm. For the Philips Achieva scanner, parameters included TE = 3.41–3.59 ms, TR = 7.46–7.77 ms, flip angle = 8° , matrix = 224×224 to 224×280 , 224–250 slices, and slice thickness = 1.1 mm.

Architecture of Deep Transfer learning models

We utilized popular pre-trained convolutional neural network (CNN) models, including AlexNet,[7] VGG19,[8] ResNet,[9] Inception,[10] GoogleNet,[11] MobileNet,[12] and DenseNet,[13] for feature extraction. This standard transfer learning strategy involves using pre-trained CNN models on ImageNet as the backbone of the model to capture generic and domain-specific features, followed by fine-tuning the top layers to learn new specialized representations tailored to our output classifier.[14] During the fine-tuning phase, the weights and biases of the CNN models were frozen to prevent changes. Due to differences in the CNN architectural designs, an adaptive pooling operation was applied to AlexNet and MobileNet before the final classification layer to ensure that the output became a one-dimensional vector. Subsequently, a new fully connected layer, the classification layer, was added to process the outputs from the hidden layer's activation function and compose the final classification. Data augmentation with random rotation and flipping was executed to improve the model training efficiency.[15] The loss function was binary cross-entropy with

logit loss. The optimizer was Adam with a learning rate of 1×10^{-4} . A total of 100 epochs with a batch size of 64 images were set for training. The validation performance was used to determine when to stop the training. The CNN models were trained until there was no improvement in the validation loss for 20 consecutive epochs. All the experiments were conducted by dividing the data into 80% for training and validation and 20% for held-out testing. A five-fold cross-validation approach was used to validate the model's performance during training. The training validation results were obtained through this five-fold cross-validation process to detect language improvements. The four-performance metrics were utilized to evaluate the model's performance in classification including the area under the receiver operating characteristic curve (AUC), accuracy (ACC), sensitivity, and specificity.

Joint domain adaption optimization

To address feature shift, a joint domain adaption optimizer was applied (see Figure S1). [16] This optimizer combined adversarial learning (via a discriminator) to extract domain-invariant features, CORAL (Correlation Alignment) to match second-order statistics (covariances) across domains, maximum classifier discrepancy (MCD) to align the discrepancies between the outputs of two classifiers, and supervised learning to minimize the classification loss. Initially, a source-led model is pretrained using labeled source and unlabeled target data, with performance evaluated on the source test set; this involves simultaneously training a feature extractor, discriminator, and two classifiers by minimizing a joint loss comprising CORAL, discriminator, discrepancy, and source classification losses. The pretrained model then generates adaptive predictions as initial pseudo-labels for target samples. Subsequently, target-led models are fine-tuned using source data and these pseudo-labeled target samples, with performance assessed on the target test set; specifically, the target feature extractor and classifier are optimized via continual backpropagation to mitigate plasticity loss, while keeping source components frozen. During continual screening and

evolving phases, they are trained by minimizing a joint loss including discriminator, CORAL, discrepancy, and target classification losses.

Here, the domain discriminator loss is defined as:

$$L_D(x_s, x_t, m) = -\mathbb{E}_{x_s \sim x_s} [\text{Log } D(m_s(x_s))] - \mathbb{E}_{x_t \sim x_t} [\text{Log } (1 - D(m_t(x_t)))]$$

Where $D(\cdot)$ is the domain discriminator, $m_s(\cdot)$ is the source feature extractor, $m_t(\cdot)$ is the target feature extractor and x is the source or target image.

Next, Coral loss (second-order alignment) was donated as:

$$L_C(x_s, x_t, m) = \frac{1}{4d^2} \sum_{i=1}^d \sum_{j=1}^d (\text{Cov}(m_s(x_s)) - \text{Cov}(m_t(x_t)))^2$$

Where, $\text{Cov}(\cdot)$ represents the computation of covariance matrix.

Meanwhile, discrepancy loss between the predictions of two classifiers is usually:

$$L_P(C_s, C_t; x) = \frac{1}{N} \sum_{i=1}^N |\sigma(C_s(m_s(x_s))) - \sigma(C_t(m_t(x_t)))|$$

Where $C_s(\cdot)$ is the source classifier, $C_t(\cdot)$ is the target classifier, and σ is the sigmoid function.

Finally, the classification loss is defined as:

$$L_{cls}^{(n)} = -\mathbb{E}_{(x,y) \sim D^{(n)}} \sum_{k=1}^K 1_{[k=y]} \text{Log } C_n(m_n(x))$$

Where $D^{(\cdot)}$ refers to the source or target data distributions.

In summary, the source-led pretrained model learns domain-invariant representations through joint domain adaptation optimization, thereby generating adaptive target predictions that serve as initial pseudo-labels for the target domain. During the screening and evolving learning phases, the target-column parameters are maintained close to the frozen source-column parameters via joint domain adaptation optimization, facilitating knowledge transfer from the source to the target domain. Consequently, the target-led models in the screening and evolving processes are iteratively trained to identify candidate subsets from the original target samples and to update the pseudo-label variants, respectively.

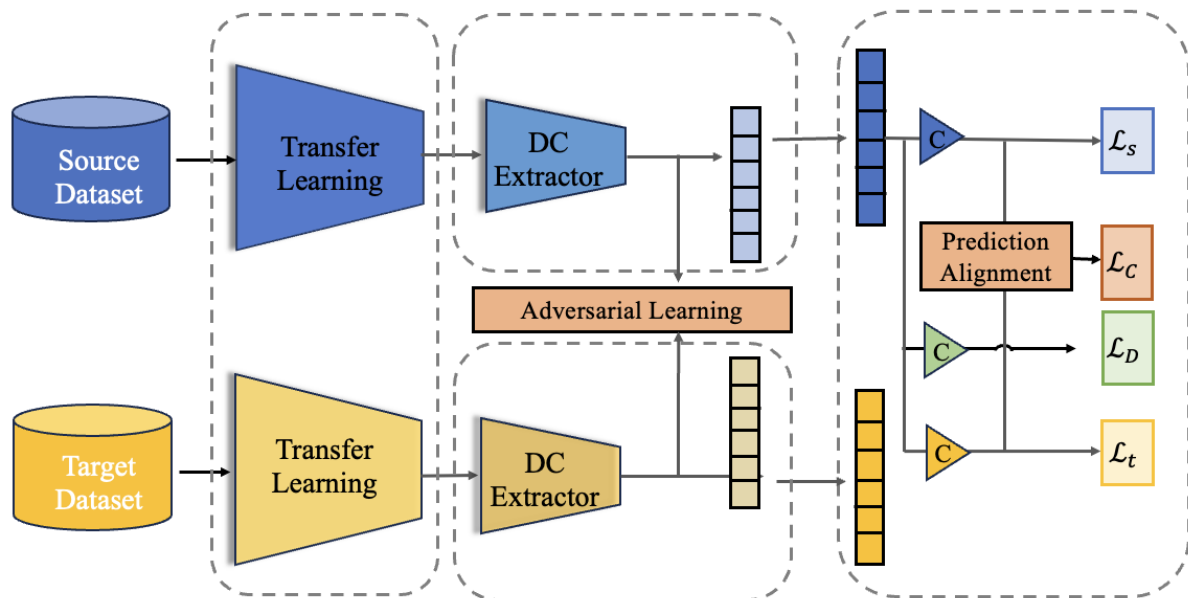


Figure S1. Illustration of the basic framework of the deep transfer learning with the joint domain adaption optimization.

Table S1. The classification performance of the deep transfer learning models in the Chicago English group.

Models	% (95% CI)			AUC (95% CI)
	Accuracy	Sensitivity	Specificity	
VGG19_bn	81.17 (80.11-82.22)	86.19 (84.80-87.57)	75.73 (73.55-77.90)	0.810 (0.799-0.820)
ResNet-50d	88.02 (86.92-89.11)	88.16 (85.98-90.34)	87.86 (86.21-89.51)	0.880 (0.869-0.891)
DenseNet_169	89.09 (88.06-90.12)	92.11 (91.47-92.74)	85.83 (83.64-88.02)	0.890 (0.879-0.900)
AlexNet	79.95 (78.61-81.30)	84.13 (82.67-85.58)	75.44 (72.53-78.35)	0.800 (0.786-0.813)
Inception_V3	83.64 (81.75-85.53)	85.65 (77.40-93.90)	81.46 (73.24-89.67)	0.836 (0.817-0.854)
GoogleNet	87.13 (85.54-88.72)	92.38 (90.53-94.22)	81.46 (79.07-83.84)	0.869 (0.853-0.885)
MobileNet	90.91 (89.41-92.41)	92.56 (90.56-94.55)	89.13 (86.97-91.28)	0.908 (0.893-0.923)

Table S2. The performance of the Transfer Learning method within and across datasets using MobileNet model.

Datasets		% (95% CI)			AUC (95% CI)
		Accuracy	Sensitivity	Specificity	
Single Dataset	Chicago_English	90.91 (89.41-92.41)	92.56 (90.56-94.55)	89.13 (86.97-91.28)	0.908 (0.893-0.923)
	Melbourne_English	94.40 (92.85-95.96)	95.17 (93.47-96.87)	93.66 (89.07-98.25)	0.944 (0.929-0.959)
	Chicago_Spanish	95.32 (94.38-96.25)	95.69 (93.65-97.72)	95.00 (92.93-97.07)	0.952 (0.944-0.963)
Combined Dataset	Chicago+Melbourne	87.59 (87.12-88.05)	86.45 (81.81-91.07)	88.83 (84.42-93.24)	0.876 (0.872-0.880)
	Chicago+Melbourne+Hong Kong	87.12 (86.05-88.19)	88.04 (84.99-91.09)	86.24 (84.46-88.02)	0.871 (0.860-0.882)
Across Center	Melbourne_English*	50.95 (49.14-52.75)	62.90 (3.74-100)	39.28 (0-95.66)	0.511 (0.489-0.533)
Across Language	Chicago_Spanish*	50.27 (46.78-53.76)	36.89 (0-93.88)	63.95 (6.43-100)	0.499 (0.467-0.532)
Across Center & Language	Hong Kong_Cantonese*	50.75 (47.62-53.87)	36.67 (0-96.18)	63.26 (3.46-100)	0.500 (0.496-0.504)

*The external validation across different languages or centers was conducted on a trained model on a single dataset (Chicago English) separately.

Table S3. The performance of the deep transfer learning with domain adaption on source dataset and various target datasets.

Datasets		% (95% CI)			AUC (95% CI)
		Accuracy	Sensitivity	Specificity	
Cross center	Source dataset (Chicago_English)	84.09 (83.32-84.87)	85.54 (82.70-88.38)	82.67 (79.65-85.68)	0.841 (0.833-0.849)
	Target dataset (Melbounre_English)	43.81(38.32-49.31)	46.15 (40.74-51.57)	41.54(33.75-49.33)	0.438(0.383-0.493)
Cross language	Source dataset (Chicago_English)	85.48 (84.62-86.35)	85.16 (82.67-87.66)	85.80 (83.87-87.72)	0.855 (0.846-0.863)
	Target dataset (Chicago_Spanish)	55.50 (43.52-67.74)	57.25 (40.26-74.25)	54.00 (45.39-62.61)	0.556 (0.433-0.677)
Cross center & language	Source dataset (Chicago_English)	86.28 (85.40-87.17)	87.46 (85.80-89.12)	85.13 (82.46-87.80)	0.863 (0.854-0.872)
	Target dataset (Hongkong_Cantonese)	53.73 (34.43-73.02)	62.61 (40.81-84.30)	46.43 (25.39-67.46)	0.545 (0.352-0.738)

Table S4. The performance of the DEM on source dataset and various target datasets.

Datasets		Phase	% (95% CI)			AUC (95% CI)
			Accuracy	Sensitivity	Specificity	
Cross center	Source dataset (Chicago_English)	-	86.88 (84.58-89.17)	83.94 (73.27-94.61)	89.46 (82.40-96.52)	0.869 (0.846-0.892)
	Target dataset (Melbounre_English)	Screening phase	62.71(59.12-66.30)	28.35(13.80-42.90)	92.24(84.38-100)	0.603(0.561-0.645)
		Evolving phase	70.73 (68.42-73.03)	49.32 (45.13-53.51)	89.18 (83.43-94.92)	0.692 (0.669-0.716)
Cross language	Source dataset (Chicago_English)	-	78.13 (73.79-82.46)	75.16 (64.33-85.97)	81.51 (74.54-88.47)	0.783 (0.742-0.830)
	Target dataset (Chicago_Spanish)	Screening phase	65.94 (53.26-78.62)	35.87 (8.23-63.51)	91.69 (84.96-98.42)	0.639 (0.533-0.786)
		Evolving phase	79.06 (66.07-92.05)	61.15 (38.70-83.59)	94.75 (87.06-100)	0.779 (0.650-0.909)
Cross center & language	Source dataset (Chicago_English)	-	64.38 (55.99-72.76)	65.40 (49.87-80.92)	63.24 (52.82-73.67)	0.644 (0.560-0.728)
	Target dataset (Hongkong_Cantonese)	Screening phase	80.00 (72.62-87.38)	83.33 (65.79-100)	77.04 (64.28-89.80)	0.802 (0.726-0.878)
		Evolving phase	83.13 (74.43-91.85)	86.67 (73.28-100)	80.00 (65.24-94.76)	0.833 (0.747-0.920)

Table S5. Performance comparisons between deep learning frameworks.

Methods	Scores	Source dataset (Chicago_English)	Target dataset (Melbourne_English)
RL	Accuracy	51.48 (49.97-52.99)	67.27 (59.92-74.66)
	Sensitivity	44.03 (12.56-75.49)	50.41 (15.94-84.89)
	Specificity	57.98 (28.11-87.86)	81.85 (61.29-100)
	AUC (95% CI)	0.510 (0.491-0.530)	0.661 (0.572-0.750)
CRL with adaptive CL	Accuracy	86.88 (84.58-89.17)	70.73 (68.42-73.03)
	Sensitivity	83.94 (73.27-94.61)	49.32 (45.13-53.51)
	Specificity	89.46 (82.40-96.52)	89.18 (83.43-94.92)
	AUC (95% CI)	0.869 (0.846-0.892)	0.692 (0.669-0.716)

Abbreviations: EWC, elastic weight consolidation;

Table S6. Performance comparisons between various reinitialization strategies.

Methods	Scores	Source dataset (Chicago_English)	Target dataset (Melbourne_English)
CRL training from scratch	Accuracy	65.53 (54.40-76.85)	66.27 (58.31-74.24)
	Sensitivity	70.20 (64.22-76.18)	70.83 (52.52-89.12)
	Specificity	63.48 (42.19-84.76)	62.22 (44.29-80.15)
	AUC (95% CI)	0.668 (0.590-0.747)	0.663 (0.583-0.742)
CRL with continual reinitialization	Accuracy	70.70 (66.99-74.41)	69.48 (61.08-77.88)
	Sensitivity	68.05 (49.85-86.26)	65.40 (49.87-80.92)
	Specificity	73.11 (58.24-87.98)	63.24 (52.82-73.67)
	AUC (95% CI)	0.706 (0.670-0.744)	0.643 (0.557-0.729)
CRL with adaptive reinitialization	Accuracy	86.88 (84.58-89.17)	70.73 (68.42-73.03)
	Sensitivity	83.94 (73.27-94.61)	49.32 (45.13-53.51)
	Specificity	89.46 (82.40-96.52)	89.18 (83.43-94.92)
	AUC (95% CI)	0.869 (0.846-0.892)	0.692 (0.669-0.716)

Table S7. Performance comparisons between random state and probability mapping mechanisms.

Methods	Scores	Source dataset (Chicago_English)	Target dataset (Melbounre_English)
DEM without confidence calibration*	Accuracy	86.64 (83.66-89.62)	68.96 (67.62-70.30)
	Sensitivity	88.71 (81.73-95.70)	46.45 (37.00-55.90)
	Specificity	84.64 (73.04-96.24)	88.43 (81.33-95.53)
	AUC (95% CI)	0.866 (0.840-0.893)	0.674 (0.656-0.693)
DEM with confidence calibration	Accuracy	86.88 (84.58-89.17)	70.73 (68.42-73.03)
	Sensitivity	83.94 (73.27-94.61)	49.32 (45.13-53.51)
	Specificity	89.46 (82.40-96.52)	89.18 (83.43-94.92)
	AUC (95% CI)	0.869 (0.846-0.892)	0.692 (0.669-0.716)

*Utilizing fixed filtering mechanism for screening learning and random mutation manner for evolving learning

References

- [1] K. E. Krasileva, S. J. Sanders, and V. H. Bal, "Peabody Picture Vocabulary Test: Proxy for verbal IQ in genetic studies of autism spectrum disorder," *Journal of autism and developmental disorders*, vol. 47, pp. 1073-1085, 2017.
- [2] I. L. Zimmerman, V. G. Steiner, and R. E. Pond, "Preschool language scale," 1979.
- [3] M. P. Bagatto, C. L. Brown, S. T. Moodie, and S. D. Scollie, "External validation of the LittleEARS® Auditory Questionnaire with English-speaking families of Canadian children with normal hearing," *International journal of pediatric otorhinolaryngology*, vol. 75, no. 6, pp. 815-817, 2011.
- [4] H. Liu, X. Jin, Y. Zhou, J. LI, L. Liu, and X. NI, "Assessment and Monitoring of the LittleEARS? Auditory Questionnaire Used for Young Hearing Aid Users in Auditory Speech Development," *Journal of Audiology and Speech Pathology*, pp. 291-294, 2015.
- [5] N. J. Tustison *et al.*, "The ANTsX ecosystem for quantitative biological and medical imaging," *Scientific reports*, vol. 11, no. 1, p. 9068, 2021.
- [6] C. Gaser, I. Nenadic, B. R. Buchsbaum, E. A. Hazlett, and M. S. Buchsbaum, "Deformation-based morphometry and its relation to conventional volumetry of brain lateral ventricles in MRI," *NeuroImage*, vol. 13, no. 6, pp. 1140-1145, 2001.
- [7] A. Krizhevsky, I. Sutskever, and G. E. Hinton, "Imagenet classification with deep convolutional neural networks," *Advances in neural information processing systems*, vol. 25, 2012.
- [8] K. Simonyan, "Very deep convolutional networks for large-scale image recognition," *arXiv preprint arXiv:1409.1556*, 2014.
- [9] K. He, X. Zhang, S. Ren, and J. Sun, "Deep residual learning for image recognition," in *Proceedings of the IEEE conference on computer vision and pattern recognition*, 2016, pp. 770-778.
- [10] C. Szegedy, V. Vanhoucke, S. Ioffe, J. Shlens, and Z. Wojna, "Rethinking the inception architecture for computer vision," in *Proceedings of the IEEE conference on computer vision and pattern recognition*, 2016, pp. 2818-2826.
- [11] C. Szegedy *et al.*, "Going deeper with convolutions," 2015, pp. 1-9.
- [12] A. G. Howard, "Mobilenets: Efficient convolutional neural networks for mobile vision applications," *arXiv preprint arXiv:1704.04861*, 2017.
- [13] G. Huang, Z. Liu, L. Van Der Maaten, and K. Q. Weinberger, "Densely connected convolutional networks," in *Proceedings of the IEEE conference on computer vision and pattern recognition*, 2017, pp. 4700-4708.
- [14] J. Yosinski, J. Clune, Y. Bengio, and H. Lipson, "How transferable are features in deep neural networks?," *Advances in neural information processing systems*, vol. 27, 2014.
- [15] A. M. Taqi, A. Awad, F. Al-Azzo, and M. Milanova, "The impact of multi-optimizers and data augmentation on TensorFlow convolutional neural network performance," in *2018 IEEE Conference on Multimedia Information Processing and Retrieval (MIPR)*, 2018: IEEE, pp. 140-145.
- [16] E. Tzeng, J. Hoffman, K. Saenko, and T. Darrell, "Adversarial discriminative domain adaptation," in *Proceedings of the IEEE conference on computer vision and pattern recognition*, 2017, pp. 7167-7176.